

The Common Intermediates of Oxygen Evolution and Dissolution Reactions during Water Electrolysis on Iridium

Olga Kasian,* Jan-Philipp Grote, Simon Geiger, Serhiy Cherevko, and Karl J. J. Mayrhofer

Abstract: Understanding the pathways of catalyst degradation during the oxygen evolution reaction is a cornerstone in the development of efficient and stable electrolyzers, since even for the most promising Ir based anodes the harsh reaction conditions are detrimental. The dissolution mechanism is complex and the correlation to the oxygen evolution reaction itself is still poorly understood. Here, by coupling a scanning flow cell with inductively coupled plasma and online electrochemical mass spectrometers, we monitor the oxygen evolution and degradation products of Ir and Ir oxides *in situ*. It is shown that at high anodic potentials several dissolution routes become possible, including formation of gaseous IrO_3 . On the basis of experimental data, possible pathways are proposed for the oxygen-evolution-triggered dissolution of Ir and the role of common intermediates for these reactions is discussed.

The oxygen evolution reaction (OER) plays a crucial role in the development of efficient electrolyzers for energy conversion and storage.^[1] The sluggish kinetics^[2] of this reaction and instability of most of the catalyzing materials^[3] remain serious challenges for the optimization of the existing technology towards cost-competitive commercialization.^[4] Currently, proton-exchange membrane water electrolyzers rely on iridium-based materials, providing a compromising combination of relatively high catalytic activity and durability.^[5] However, even Ir-based anodes slowly undergo dissolution under operation conditions of the OER.^[6] Considering the low abundance and high price of Ir, understanding the kinetics and mechanism of its electrochemical dissolution is of

high importance for a knowledge-based improvement of performance.^[7] Kinetic parameters of the Ir dissolution reaction can be determined by electrochemical methods^[8] or more directly by utilizing sensitive analytical methods such as, for example, inductively coupled plasma mass spectrometry (ICP-MS).^[9] Mechanistic studies of both OER and dissolution at the solid–liquid interface are more challenging, as they typically require detection of reaction intermediates with short lifetimes. Since experimental data on intermediates have been inaccessible so far, possible mechanisms are the subject of intensive debate in the literature.^[7,10] Most of the proposed pathways of OER on metallic Ir and its oxides were based on measurements on hydrous or anodically formed oxide films. A recent OER mechanism in acidic media suggested in a number of studies^[7,11] includes the participation of Ir^{III} species, which are considered crucial for high activity. During anodic polarization of hydrous oxide in acid^[12] $\text{Ir}^{\text{III}}\text{--Ir}^{\text{V}}$ oxidation state switching was also shown to occur. The formation of Ir^{V} and Ir^{III} intermediates during OER was confirmed experimentally by application of XAS^[12] and XPS-based techniques.^[13] Additionally, the OER on IrO_2 nanoparticles was suggested to proceed via $\text{Ir}^{\text{IV}}\text{--Ir}^{\text{V}}$ transformation.^[13a] The role of the abovementioned intermediates for the stability of Ir, however, was not discussed in this work. In our previous study using the data on the dissolution rates of metallic Ir and hydrous Ir oxide, stability was suggested to correlate to the activity and thus the $\text{Ir}^{\text{III}}\text{--Ir}^{\text{V}}$ transformation was proposed.^[9,14] Interestingly, another possible route for OER-triggered Ir degradation was suggested to occur via formation of volatile iridium species in the Ir^{VI} oxidation state, assuming similarities between Ir and Ru.^[15] Specifically, Kötz et al. proposed such a route based on the data of Wohlfahrt-Mehrens and Heitbaum, who showed with the aid of differential or online electrochemical mass spectrometry (DEMS/OLEMS) that Ru dissolves via the formation of volatile RuO_4 during OER.^[16] DEMS- and OLEMS-based techniques were also utilized to shed some light on the mechanism of OER on Pt,^[17] Ru,^[18] IrO_2 ,^[19] and non-noble perovskites;^[2] however, dissolution was out of the scope of these studies and formation of volatile Ir oxides during the OER has not yet been confirmed experimentally.

Here we utilized a scanning flow cell (SFC) coupled with OLEMS to further resolve the degradation pathway of metallic Ir and its oxides (thermally formed or reactively sputtered) and the correlation to the OER mechanism. The high sensitivity of our setup allows us to detect minor amounts of volatile products. Additionally, the activity and stability of these electrodes are investigated in parallel by a SFC connected to ICP-MS (see arrangement of setups in Figure S1).

[*] Dr. O. Kasian, Dr. J.-P. Grote, Dr. S. Geiger, Dr. S. Cherevko, Prof. K. J. J. Mayrhofer
Max-Planck-Institut für Eisenforschung GmbH
Max-Planck-Strasse 1, 40237 Düsseldorf (Germany)
E-mail: o.kasian@mpie.de

Dr. S. Cherevko, Prof. K. J. J. Mayrhofer
Helmholtz-Institute Erlangen-Nürnberg for Renewable Energy
IEK-11, Forschungszentrum Jülich GmbH
Egerlandstrasse 3, 91058 Erlangen (Germany)

Prof. K. J. J. Mayrhofer
Department of Chemical and Biological Engineering
Friedrich-Alexander-Universität Erlangen-Nürnberg
Egerlandstrasse 3, 91058 Erlangen (Germany)

Supporting information and the ORCID identification number(s) for the author(s) of this article can be found under:
<https://doi.org/10.1002/anie.201709652>.

© 2018 The Authors. Published by Wiley-VCH Verlag GmbH & Co. KGaA. This is an open access article under the terms of the Creative Commons Attribution Non-Commercial License, which permits use, distribution and reproduction in any medium, provided the original work is properly cited, and is not used for commercial purposes.

Details regarding the electrode preparation and characterization are presented and discussed in the Supporting Information. In short, the composition of the as-prepared metallic Ir film and its oxides was confirmed using X-ray photoelectron spectroscopy (Figures S2–S4). Both reactively sputtered and thermally formed oxides consist of IrO₂ only (Figures S3 and S4), while the as-prepared Ir film shows only a metallic phase (Figure S2). Considering that the evolution of oxygen always results in oxidation of the electrode, the term “metallic Ir electrode” refers to an electrochemically formed oxide formed during short-term polarization.

The summarized data on the stability of the thermally formed Ir oxide (thermal oxide) is exemplarily presented in Figure 1. The electrode is polarized at 5, 10, 15, and

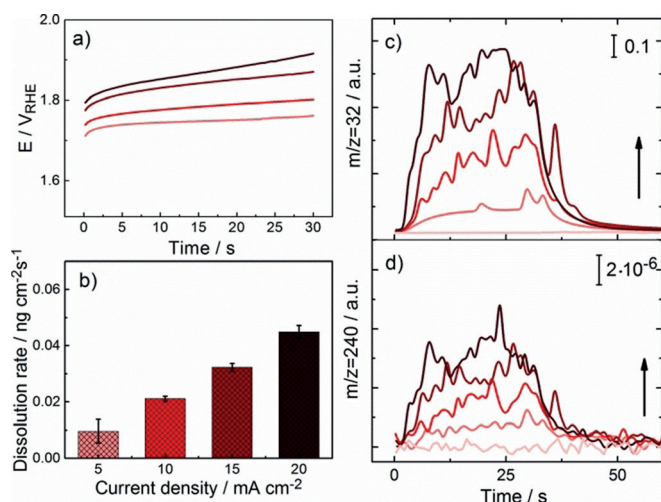


Figure 1. a) Measured potential during 30 s of anodic polarization of Ir thermal oxide in 0.1 M HClO₄ at 5, 10, 15, and 20 mA cm⁻² at room temperature. b) Average rate of iridium dissolution as measured online with ICP-MS. Mass spectra of c) O₂ (*m/z* 32) and d) IrO₃ (*m/z* 240) acquired online with OLEMS. The color gradient indicates the increase of applied current density from 5 mA cm⁻² to 20 mA cm⁻². The baselines in (c) and (d) show the O₂ (*m/z* 32) and IrO₃ (*m/z* 240) signals measured at the open circuit potential.

20 mA cm⁻² during 30 s and the corresponding values of potential (a) and the average dissolution rate of Ir (b) are measured online. Simultaneously, the volatile species with mass-to-charge ratios (*m/z*) of 32 (c) and 240 (d) formed during the OER are measured in situ (see Figures 1 and S5). In line with dissolution, the formation of O₂ and IrO₃ becomes more pronounced at higher current densities (Figure 1c,d). Metallic Ir and reactively sputtered oxide show the same trend and increase in both dissolution and IrO₃ formation with increasing current density (see Figures S6 and S7, respectively). For thermal oxide, formation of IrO₃ is observed already at 5 mA cm⁻², while the evolution of this volatile intermediate on metallic Ir and reactively sputtered IrO₂ is negligible or even absent at low current densities.

Considering the OER as the main anodic reaction on iridium oxides, polarization of different electrodes at the same current density leads to an equal amount of evolved O₂. However, at the identical current density conditions both the

stability and the formation of IrO₃ strongly depend on the nature of the Ir anode, as well as on the different values of potential imposed by these electrodes.

For a semiquantitative estimation of the interplay between the activity and the formation of IrO₃, the integrated signal of *m/z* 240 and the value of potential at the end of polarization were plotted versus applied current density (Figure 2b,c). Both dissolution of Ir and formation of volatile

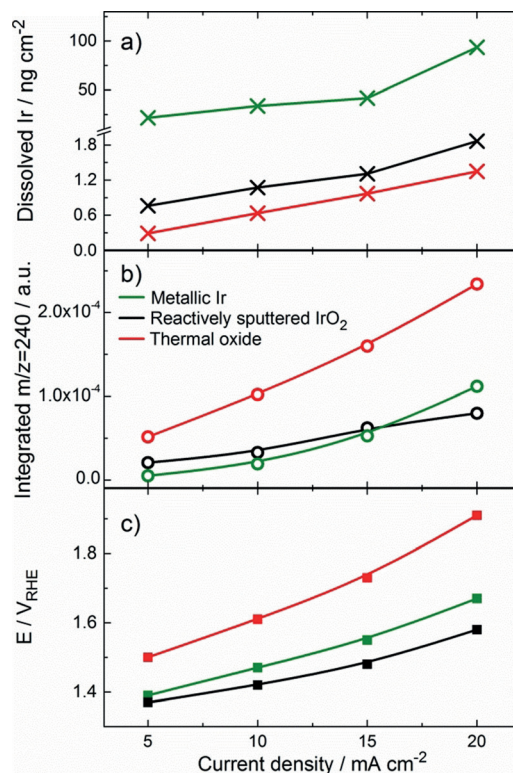


Figure 2. Dependence of a) the amount of dissolved Ir, b) the formation of IrO₃ and potential at the end of polarization on the current density obtained for metallic Ir (green), reactively sputtered IrO₂ (black) and thermal IrO₂ (red).

IrO₃ clearly depend on the value of applied current density and the nature of the electrode. At high current densities, dissolution of metallic Ir is about two orders of magnitude higher than for thermal or reactively sputtered oxides (Figure 2a). Considering the lower value of potential on metallic Ir (Figure 2c), the dominating dissolution mechanism on this electrode includes formation of intermediates in an oxidation state lower than Ir^{VI}, for example, Ir^{III} or Ir^V. During anodic polarization metallic Ir⁰ can undergo direct dissolution forming soluble Ir³⁺ and further transform to IrO₂ [see Scheme 1, Eqs. (S1) and (S2)]. Additional dissolution of metallic Ir beneath the non-uniform oxide film is also possible. One should consider, however, that direct dissolution Ir⁰–Ir³⁺ becomes less favorable with increasing oxide coverage on the metal surface and obviously does not occur on thermal or reactively sputtered oxides. Consequently, reactively sputtered IrO₂ with similar electrocatalytic activity to metallic Ir is significantly less prone to dissolution. the superior electrocatalytic behavior of reactively sputtered IrO₂

order to increase the selectivity towards the desired product. In this context we believe that the presented fundamental results can help guide the development of more stable oxygen evolution electrocatalysts.

Acknowledgements

O.K. acknowledges the Alexander von Humboldt Foundation. We acknowledge the MAXNET Energy research initiative of the Max Planck Society for financial support. S.C. and K.J.J.M. acknowledge funding by the German Federal Ministry of Education and Research (BMBF) within the Kopernikus Project P2X.

Conflict of interest

The authors declare no conflict of interest.

Keywords: electrochemical mass spectrometry · iridium dissolution · oxygen evolution reaction · reaction mechanisms · water electrolysis

How to cite: *Angew. Chem. Int. Ed.* **2018**, *57*, 2488–2491
Angew. Chem. **2018**, *130*, 2514–2517

- [1] V. R. Stamenkovic, D. Strmcnik, P. P. Lopes, N. M. Markovic, *Nat. Mater.* **2017**, *16*, 57–69.
- [2] A. Grimaud, O. Diaz-Morales, B. Han, W. T. Hong, Y.-L. Lee, L. Giordano, K. A. Stoerzinger, M. T. M. Koper, Y. Shao-Horn, *Nat. Chem.* **2017**, *9*, 457–465.
- [3] T. Binninger, R. Mohamed, K. Waltar, E. Fabbri, P. Levecque, R. Kotz, T. J. Schmidt, *Sci. Rep.* **2015**, *5*, 12167.
- [4] Z. W. Seh, J. Kibsgaard, C. F. Dickens, I. Chorkendorff, J. K. Nørskov, T. F. Jaramillo, *Science* **2017**, *355*, eaad4998.
- [5] a) G. Beni, L. M. Schiavone, J. L. Shay, W. C. Dautremont-Smith, B. S. Schneider, *Nature* **1979**, *282*, 281–283; b) O. Diaz-Morales, S. Raaijman, R. Kortlever, P. J. Kooyman, T. Wezendonk, J. Gascon, W. T. Fu, M. T. M. Koper, *Nat. Commun.* **2016**, *7*, 12363; c) L. C. Seitz, C. F. Dickens, K. Nishio, Y. Hikita, J. Montoya, A. Doyle, C. Kirk, A. Vojvodic, H. Y. Hwang, J. K. Nørskov, T. F. Jaramillo, *Science* **2016**, *353*, 1011–1014.
- [6] a) S. Cherevko, S. Geiger, O. Kasian, N. Kulyk, J.-P. Grote, A. Savan, B. R. Shrestha, S. Merzlikin, B. Breitbach, A. Ludwig, K. J. J. Mayrhofer, *Catal. Today* **2016**, *262*, 170–180; b) O. Kasian, S. Geiger, P. Stock, G. Polymeros, B. Breitbach, A. Savan, A. Ludwig, S. Cherevko, K. J. J. Mayrhofer, *J. Electrochem. Soc.* **2016**, *163*, F3099–F3104; c) N. Danilovic, R. Subbaraman, K.-C. Chang, S. H. Chang, Y. J. Kang, J. Snyder, A. P. Paulikas, D. Strmcnik, Y.-T. Kim, D. Myers, V. R. Stamenkovic, N. M. Markovic, *J. Phys. Chem. Lett.* **2014**, *5*, 2474–2478.
- [7] T. Reier, H. N. Nong, D. Teschner, R. Schlögl, P. Strasser, *Adv. Energy Mater.* **2017**, *7*, 1601275.
- [8] A. Damjanovic, A. Dey, J. O. M. Bockris, *J. Electrochem. Soc.* **1966**, *113*, 739–746.
- [9] S. Cherevko, S. Geiger, O. Kasian, A. Mingers, K. J. J. Mayrhofer, *J. Electroanal. Chem.* **2016**, *773*, 69–78.
- [10] C. Spöri, J. T. H. Kwan, A. Bonakdarpour, D. P. Wilkinson, P. Strasser, *Angew. Chem. Int. Ed.* **2017**, *56*, 5994–6021; *Angew. Chem.* **2017**, *129*, 6088–6117.
- [11] V. Pfeifer, T. E. Jones, J. J. Velasco Velez, C. Massue, M. T. Greiner, R. Arrigo, D. Teschner, F. Girgsdies, M. Scherzer, J. Allan, M. Hashagen, G. Weinberg, S. Piccinin, M. Havecker, A. Knop-Gericke, R. Schlögl, *Phys. Chem. Chem. Phys.* **2016**, *18*, 2292–2296.
- [12] A. Minguzzi, O. Lugaesi, E. Achilli, C. Locatelli, A. Vertova, P. Ghigna, S. Rondinini, *Chem. Sci.* **2014**, *5*, 3591–3597.
- [13] a) H. G. Sanchez Casalongue, M. L. Ng, S. Kaya, D. Friebe, H. Ogasawara, A. Nilsson, *Angew. Chem. Int. Ed.* **2014**, *53*, 7169–7172; *Angew. Chem.* **2014**, *126*, 7297–7300; b) V. Pfeifer, T. E. Jones, J. J. Velasco Vélez, C. Massué, R. Arrigo, D. Teschner, F. Girgsdies, M. Scherzer, M. T. Greiner, J. Allan, M. Hashagen, G. Weinberg, S. Piccinin, M. Hävecker, A. Knop-Gericke, R. Schlögl, *Surf. Interface Anal.* **2016**, *48*, 261–273.
- [14] S. Cherevko, S. Geiger, O. Kasian, A. Mingers, K. J. J. Mayrhofer, *J. Electroanal. Chem.* **2016**, *774*, 102–110.
- [15] R. Kötz, H. Neff, S. Stucki, *J. Electrochem. Soc.* **1984**, *131*, 72–77.
- [16] M. Wohlfahrt-Mehrens, J. Heitbaum, *J. Electroanal. Chem.* **1987**, *237*, 251–260.
- [17] O. W. J. Willsau, J. Heitbaum, *J. Electroanal. Chem. Interfacial Electrochem.* **1985**, *195*, 299–306.
- [18] K. Macounova, M. Makarova, P. Krtil, *Electrochem. Commun.* **2009**, *11*, 1865–1868.
- [19] S. Fierro, T. Nagel, H. Baltruschat, C. Cominellis, *Electrochem. Commun.* **2007**, *9*, 1969–1974.
- [20] J. O. Bockris, *J. Chem. Phys.* **1956**, *24*, 817–827.
- [21] A. Minguzzi, C. Locatelli, O. Lugaesi, E. Achilli, G. Cappelletti, M. Scavini, M. Coduri, P. Masala, B. Sacchi, A. Vertova, P. Ghigna, S. Rondinini, *ACS Catal.* **2015**, *5*, 5104–5115.
- [22] J. D. E. McIntyre, S. Basu, W. F. Peck, W. L. Brown, W. M. Augustyniak, *Phys. Rev. B* **1982**, *25*, 7242–7254.
- [23] A. Grimaud, A. Demortière, M. Saubanière, W. Dachraoui, M. Duchamp, M.-L. Doublet, J.-M. Tarascon, *Nat. Energy* **2016**, *2*, 16189.

Manuscript received: September 18, 2017

Accepted manuscript online: December 8, 2017

Version of record online: February 5, 2018